# Preparation and Characterization of Betacyclodextrin doped Nanosize Poly(o-toluidine)

**B. Mahalakshmi, C. Vedhi**
Department of Chemistry, V.O. Chidambaram College, Thoothukudi, India
Email: maha.adithya@gmail.com, cvedhi23@gmail.com

## Abstract

Surfactant doped Poly (o-toluidine) (POT) was synthesized in an aqueous solution of o-toluidine and non-ionic surfactant of Betacyclodextrin (BCD) by chemical method by varying the o-toluidine to surfactant ratio. The role of doping on the structure and morphological changes in poly (o-toluidine) were characterized by FTIR, UV-Visible spectroscopy, cyclic voltammetric (CV), SEM, TGA, XRD, TEM and electrochemical impedance spectroscopy measurements and the results were analyzed. The resulting polymers exhibit an enhanced solubility in solvents like DMSO, DMF, acetone, acetonitrile and THF. UV-Vis spectra display the absorbance around 800 nm assigned to polaron form of POT. The FT-IR spectra reveals that the amine vibration peak at 1598 $cm^{-1}$ is shifted to 1591 $cm^{-1}$ and it confirms the interaction of POT with BCD. The SEM micrographs shows distinct morphological features of BCD doped POT. The incorporation of BCD in POT is confirmed by EDAX. The XRD results show the particle size of POT 1 is 30 nm and in the case of POT 5 the particle size is 73 nm. Electrochemical behavior was studied by CV and exhibits one oxidation peak (385.9 mV) and one reduction peak (-109.7 mV) for BCD doped POT. Impedance spectra display POT with maximum surfactant concentration exhibits maximum conductivity. The TGA results suggest a higher thermal stability for BCD doped POT than that for the pure POT. The nano-sized polymer was confirmed by TEM image.

Keywords: Poly (o-toluidine), Betacyclodextrin, XRD, Cyclic Voltammetry, morphology.

## 1. INTRODUCTION

Conducting polymers have attracted considerable attention because of their electrical and optical properties and many potential applications such as energy storage, electromagnetic interference shielding optoelectronic device, sensors [1-7] Scientists are almost for not sparing any efforts in solving numerous problems which restricts the use of these polymers in variety of applications.

Polyaniline (PANI) is by far the most investigated conducting polymer. However, major problem related to its successful utilization lays in its poor mechanical properties and process ability due to its insoluble nature in common organic solvents [8, 9]. The common way to change the physical and chemical properties of polymer is to substitute the polymer chain with special chemical groups like –CH3, -C2H5, -OH, -OCH3 [10] etc**.** Poly toluidines have attracted considerable attention as they exhibit better solubility in many solvents and better processability than PANI [9]. MacDiarmid and coworkers [11] suggested that introduction of –CH3 substituent on the phenyl rings increases the torsion of neighboring benzene rings on the polymer chain thereby resulting in decrease in the extent of conjugation of Poly Ortho Toluidine (POT)

Better processability may be achieved either by the synthesis on PANI in nano-micro scale particle, which is easier to disperse in a polymer matrix or by using an appropriate emulsifier which enhances the optical and electrical properties of PANI. Polymeric stabilizers (surfactant) affect the polymerization condition, kinetics and also the final properties of the polymer [12,13] Surfactants have been used as an additive in the polymerization reactions for it affects the inverse emulsion pathways and it improves the properties of the polymers with respect to conductivity, stability, solubility in organic solvents, and processability. Particle size and conductivity can be decreased by increasing the concentration of stabilizer [14, 15]. These are related to the mass of insulating stabilizer adsorbed. The size and type of the dopant (anion) affect the morphology, size and electrical conductivity of resulting polymers [16, 17].

The surfactant micelles control the distribution of the reactants between the micellar and aqueous phases. Jaroslav Stejskal et al have reported that the surfactants have

been used as additives in the polymerization of aniline and pyrrole and compared their electrical and thermal properties [18]. According to Lee et. al [19] PPy chemically prepared and doped with bulky anion of dodecyl benzene sulfonic acid (DBSA) was soluble in m-cresol and after the addition of a co-surfactant such as camphor sulfonic acid, chloroform, dichloromethane and 1,1,2,2-tetrachloroethane. PANI with TritonX-100 chemical synthesis has been reported [20, 21]. In the present work, Betacyclodextrin (BCD) doped poly (o-toluidine) (POT) was synthesized by chemical oxidation of o-toluidine using KPS as an oxidizing agent in the presence of various surfactant ratios. The synthesized polymers were characterized by fourier transform infrared spectroscopy and scanning electron microscopy. The effect of doping agent on structural and morphology is investigated.

## II. EXPERIMENTAL SECTION

### 2.1. Materials

The monomer o-toluidine was purified by distillation in vacuum before use. Betacyclodextrin (BCD, surfactant), potassium peroxydisulfate (KSP, oxidant), and Hydrochloric acid, were purchased from merck AR grade and used as received.

### 2.2. Chemical preparation of poly(o-toluidine) with and without Betacyclodextrin:

To the monomer o-toluidine (0.1 M), the oxidant KSP (0.1M) and the initiator HCl (1M) were added drop wise with constant stirring and it was left for stirring for 5 hrs to complete the polymerization. The synthesized polymer was filtered, washed several times with distilled water then dried at room temperature. The POT-BCD was prepared by mixing various molar ratio of surfactant into 0.1M o-toluidine and 0.1M KSP solution. The polymerization conditions as for the synthesis of POT without surfactant. Table1 describe the synthetic conditions of the respective samples.

### 2.3. Characterization

The FT-IR spectroscopy was recorded using Model SHIMADZU FT-IR spectrometer by pelletizing polymer with KBr. The polymers were recorded in the frequency range from 400 to 4000 $cm^{-1}$. The UV- Vis spectrum of polymers was taken using JASCO-V530 dual beam spectrophotometer by dissolving the polymers in DMSO as a solvent. The morphology of the synthesized polymers were studied using JEOL model JSM-6360. The XRD was measured with XPERT-PRO diffractometer using CuK (k=1.54060) radiation. The electrochemical workstation (model 650C), CH-Instrument Inc., TX, USA was employed for performing Cyclic voltammmetry and impedance studies. The percentage solubility of the polymers were determined by weight loss method (W/V %). The particles size were studied using TEM instrument (Model: PHILIPS–CM200) operating at 20–200 kv with a resolution of 2.4 Å.

## III. RESULTS AND DISCUSSION

### 3.1. Solubility

The solubility of the betacyclodextrin (BCD) presented poly (o-toluidine) (POT 1) was studied in various solvents. Table 2 shows the percentage solubility of solvents. The percentage solubility increases with the increase of BCD content in the polymer. This behavior had more advantage for further processing of doped POT.

### 3.2. IR spectra

FT-IR spectra have been recorded for undoped and BCD doped POT are shown in Fig.1. The two main bands at 1666 and 1591 $cm^{-1}$ assigned to the ring stretching vibration of the quinoid and benzenoid rings respectively. The peak observed at 1114 $cm^{-1}$ is due to the C-H in plane bending vibration. The peaks at 883 and 811 $cm^{-1}$ corresponds to para disubstituted aromatic rings. The new band appears at 1195 $cm^{-1}$could be attributed to the $–CH_3$ rocking mode. The vibration band at 1332 $cm^{-1}$ may be due to C-N stretching and due to ring stretching vibration [22, 23]. The band at 3313, 2972, 1195 and 1400 $cm^{-1}$corresponds to the symmetric and anti symmetric stretching of ν[OH], ν[CH2] , ν[C-C] and in-plane bending vibration of ν[OH] of BCD observed in BCD doped POT respectively [24]. The POT prepared with BCD has all the peaks of polymer but the values are slightly shifted towards longer wave number. The intensity of these peaks increases with increasing the concentration of the surfactants. The change in number and intensity of IR vibrational bands confirms the dopant interaction with poly (o-toluidine).

### 3.3. UV Spectra

The UV-visible spectra of POT and POT with different concentrations of BCD used polymers are shown in fig. 2. It shows absorption around 310 and 600 nm. The peak in the UV range is assigned to $\pi$-$\pi^*$transitions, whereas the peak in the visible range is assigned to the polaronic transitions from the benzenoid ring (HOMO) to the

quinonoid ring (LUMO), i.e., from $\pi_B$-$\pi_Q$. The peak in the visible range also confirms the presence of the doped state of conducting polymer. The absorbance around 800 nm assigned to polaron form (surfactant doped POT) [25]. The peak in the visible range also confirms the presence of doped state of conducting polymer. The polymers with BCD shows two bands corresponding to $\pi$-$\pi^*$transition of benzene ring and $\pi$-$\pi^*$ transition of benzenoid and quinonoid structures and the values are considerably blue shifted which indicates the interaction between POT and the surfactant. The intensity of absorption band increases with the increasing BCD content.

### 3.4. SEM analysis

The SEM micrograph of BCD doped and undoped POT is shown in figure. 3. The undoped POT (fig. 3 a) exhibits a granular structure [26]. The morphology of POT 1 (fig. 3(b)) appeared in globular structure and POT 2 exhibit granular structure. Examination of POT 3 reveals less branching and more granules. As shown in fig. 3 (d&e) describe spherical and distorted spherical structure for POT 4 and POT 5 respectively. The variation in morphology of the doped POT was predominantly dependent on the concentration of the surfactant. Figure 4 Shows the EDS spectroscopy for the undoped and BCD doped POT. It can be seen from line **a** that for the undoped POT, only peaks corresponding to C and N elements were displayed. While for the BCD doped POT, besides above peaks, peaks corresponding to C, N and O were also clearly observed, suggesting that O element originated from BCD was doped into the polymer.

### 3.5. XRD analysis

XRD patterns of undoped and surfactant doped Poly (o-toluidine) are shown in fig. 5. XRD pattern of undoped POT sample shows an amorphous behavior and a hump around 24º and the particle size is 53nm. The particle size varies gradually from 30 nm in the case of POT 1 to 73 nm in the case of POT 5 indicating that the concentration of the surfactant is highly influenced on the size of the particles. Particle size and conductivity can be decreased by increasing the concentration of stabilizer. The variation in diffraction intensity with doped concentration exhibits with the interaction of BCD in POT network.

### 3.6. Cyclic Voltammogram

Electrochemical behavior of undoped POT and BCD doped POT are shown in Figure 6 The CVs were obtained in 0.1M $H_2SO_4$ by casting the polymer on GC working electrode and scanned between -0.6 to 1.2 V at scan rates between 25 and 500 mV/s. The undoped POT shows three oxidation peaks. The peak at 992.2 mV corresponds to the oxidation of the monomer. The peak 279.4 mV was attributed to the transformation of POT from the reduced leucoemeraldine (LE) state to the partially oxidized emeraldine state (ES) of POT. The peak at 610.6 mV due to the presence of quinine/hydroquinone [27-29]. BCD doped POT shows one redox peak occurred at approximately 385.9/-109.7 mV was attributed to the transformation of POT from the reduced leucoemeraldine state to the partially oxidized emeraldine state (ES) of POT. The cathodic and anodic peak positions of BCD doped POT shifted and increases the charge transfer with increasing the concentration of the surfactant were shown in the curve from (b-f). The effect of varying scan rate ranges between 25mV/s and 500mV/s was studied at the BCD doped POT in 0.1M $H_2SO_4$ as shown in Figure 7a. With an increasing scan rate the peak current also increased thus indicating good adherence of the polymer onto the GC electrode surface, the peak current separation increased, and also the peak potential shifted slightly with the anodic peak to positive and the cathodic peak to negative potential directions. This is because the charging and discharging of the electro-active conducting polymer is rate determining. Figure 7b shows a plot of anodic peak current against scan rate for BCD doped POT. It shows that a linear relationship between anodic peak currents versus scan rate for BCD doped POT and it indicates that the polymer has an appropriate electro activity.

### 9.7. Impedance spectra

Figure 8 shows the typical Nyquist plots of BCD doped and undoped POT in 0.1M $H_2SO_4$. The diameter of the semi-circle gives an approximate value of the charge transfer resistance ($R_{ct}$) of the POT/electrolyte interface. An $R_{ct}$ and $C_{dl}$ value of the polymer is given in the table 3. The radii of the semicircle were found to increase with decrease in the surfactant concentration. Thus POT 1 gives maximum conductivity.

### 9.8. TGA/DTA

The TGA curves for the BCD doped POT and undoped POT are shown in Fig. 9. BCD doped POT shows 4% weight loss around 100 ºCdue to the loss of water molecules /moisture. The second weight loss (19.3 wt.%)

step occurring upto 300.62ºC is attributed to the loss of loosely bounded dopant (BCD). After 465.36 ºC the polymer undergoes degradation [30]. The surfactant doped polymers thus have better thermal stability when compared to undoped polymer for which the degradation temperature is 465.36 ºC.

### 9.9. TEM

Fig. 10 shows the transmission electron micrograph of BCD doped POT. It show a fibre like structure and size of the particles found to be in nano range.

## IV. CONCLUSION

POT doped with BCD (pH=7.92) was synthesized by chemical method. The polymer was identified by UV-Vis, FT-IR, XRD, SEM and TEM. The resulting polymers exhibit an enhanced solubility in solvents like DMSO, DMF, acetone, acetonitrile and THF. UV-Vis spectra display the absorbance around 800 nm assigned to polaron form of POT. The FT-IR spectra reveals that the amine vibration peak at 1598 $cm^{-1}$ is shifted to 1591 $cm^{-1}$ and it confirms the interaction of POT with BCD. The SEM micrographs shows distinct morphological features of BCD doped POT. The incorporation of BCD in POT is confirmed by EDAX. The XRD results show the particle size of POT 1 is 30 nm and in the case of POT 5 the particle size is 73 nm. Electrochemical behavior was studied by CV and exhibits one oxidation peak (385.9 mV) and one reduction peak (-109.7 mV) for BCD doped POT. Impedance spectra display POT with maximum surfactant concentration exhibits maximum conductivity. The TGA results suggest a higher thermal stability for BCD doped POT than that for the pure POT. The nano-sized polymer was confirmed by TEM image.

**Table 1. Synthetic conditions of doped and undoped POT**

| Sample | o-toluidine(M) | KPS(M) | BCD(M) |
|---|---|---|---|
| POT | 0.1 | 0.1 | - |
| POT 1 | 0.1 | 0.1 | $1x10^{-3}$ |
| POT 2 | 0.1 | 0.1 | $8x10^{-4}$ |
| POT 3 | 0.1 | 0.1 | $2x10^{-4}$ |
| POT 4 | 0.1 | 0.1 | $8x10^{-5}$ |
| POT 5 | 0.1 | 0.1 | $2x10^{-5}$ |

**Table 2. The range of percentage solubility of BCD doped POT (POT 1- POT 5) in various solvents**

| Solvent | % solubility |
|---|---|
| DMSO | 100 |
| DMF | 100 |
| Acetone | 87-92 |
| Aceticacid | 61-65 |
| Dichloromethane | 68-71 |
| THF | 60-63 |
| Water | 34-37 |
| Toluene | 40-44 |
| Xylene | 31-33 |

**Table 3.Impedance parameters of BCD doped and undoped POT**

| polymer | $R_{ct}$ ($\Omega cm^2$) | $C_{dl}$ ($\mu F cm^{-2}$) |
|---|---|---|
| POT (pure) | 2297.8 | 0.0606 |
| POT 1 | 460.4 | 1.4862 |
| POT 2 | 716.0 | 0.6712 |
| POT 3 | 970.8 | 0.3182 |
| POT 4 | 1411.8 | 0.1856 |
| POT 5 | 1962.6 | 0.0831 |

**References:**


[1] S. M. Ahmed and S. A. Ahmed, Eur. Polym. J., vol. 32 pp. 25, 2002.

[2] S. E. Jacobo, J. C. Aphesteguy, R. L. Anton, G. V. Schegoleva and G. V. Kurlyandskaya Eur Polym J, vol. 43, pp. 1333, 2007.

[3] Y. Li, T. Kunitake and S. Fujikawa, Colloids and Surfaces, vol. 275, pp. 209, 2006.

[4] T. Taka, Synth. Met. vol. 41, pp. 1177, 1991.

[5] H. Nishino, G. Yu, A. J. Heeger, T. A. Chen and R. D. Rieke, Synth. Met., vol. 68, pp. 243, 1995.

[6] W. M. Azevedo, J. M. Souza and J. V. Melo, Synth. Met., vol. 100, pp. 241, 1999.

[7] P. N. Bartlett, M. A. Patricia and K.L.C. Sin, Sensors & Actuators, vol. 19, pp. 125, 1989.

[8] Tetsuo Hino, Takumi Namiki and Noriyuki Kuramoto, Synthetic Metals, vol. 156, pp. 1327, 2006.

[9] H. Swaruparani, S. Basavaraja, C. Basavaraja, Do Sung Huh and A.Venkataraman, Journal of Applied Polymer Science, vol. 117, pp. 1350, 2010.

[10] Milind V Kulkarn, Annamraju Kasi Viswanath and U. P. Malik, Materials Chemistry and Physics, vol. 89,pp. 1, 2005.

[11] Y Wei, W. Focke, G. E. Wnek, A. Ray and A.G. Mac Diarmid, J. Phys.Chem.**, 1989**, vol. 93, pp. 495, 1989.

[12] S. P. Armes and M. Aldissi, Journal of Chemical Society, Chemical Communications, vol. 2, pp.88, 1989.

[13] N. Kohut-Svelko, S. Reynaud and J. Francois, (2005) Synthetic Metals, vol.150, pp. 107, 2005.

[14] S. P. Armes, J. F. Miller and B. Vincent, Journal of Colloid and Interface Science, vol. 118, pp. 410, 1987.

[15] S. P. Armes and M. Aldissi, Polymer, vol.31, pp. 569, 1990.

[16] S. Hayashi, S. Takeda, K. Kaneto, K. Yoshino and T, Matsuyama, *S*ynthetic Metals, vol. 18, pp. 591, 1987.

[17] M. Tang, T. Y. Wen, T. B. Du and Y. P. Chen, (2003) European Polymer Journal, vol. 39, pp. 143, 2003.

[18] Jaroslav Stejskal, Maria Omastova, Svetlana Fedorova, Jan Prokes and Miroslava Trchova, Polymer, vol. 44, pp. 1353, 2003.

[19] J.Y. Lee, D. Y. Kim and C. Y. Kim **1995** Synthetic Metal 74 103.

[20] T. C. Girija and M. V. Sangarranarayanan, Journal of PowerSources, Vol. 159, pp. 1519 2006.

[21] N. Arsalani, M. Khavei and A. A. Entezami, Iranian Polymer Journal, Vol. 12, pp.237, 2003.

[22] G.B. V. S. Lakshmi, V. Ali, A. M. Siddiqui, P. K. Kulriya, M. Hasain and M. Zulfequar, Phys. B., vol. 392, pp. 259, 2007.

[23] N.D. Singho, N. A. C. Lah, M. R. Johan and R. Ahmad, Int. J. Electrochem. Sci., 2012, vol.7, pp. 5596, 2012.

[24] Kavirajaapandiansambasevam, SharifahMohamad, NorazilawatiMuhamadsarih and Nor Atiqah Ismail, Int. J. Mol. Sci., vol. 14, pp. 3671, 2013.

[25] C. Ozdemir, H. Can, N. Kolac, A. Guner, J. App. Polym. Sci., vol. 99, pp. 2182, 2006.

[26] K.S. Ryu, K.M. Kim, S.G. Kang, G. J. Lee, J. Joo and S. H. Chang, Synth. Met., vol. 110, pp. 213, 2000.

[27] A. Talei, J.Y. Lee, Y.K. Lee, J. Jang, J.A. Romagnoli, T. Taguchi and E. Maeder, Thin Solid Films, vol. 363, pp. 163, 2000.

[28] A. Kumar, D.M. Welsh, M.C. Morvant, F. Piroux, K.A. Abboud and J.R. Reynolds, Chem. Mater., vol. 10, pp. 896, 1998.

[29] J.C. Scott, S. A. Carter, S. Karg and M. Angelopoulos, Synth. Met., vol. 85, pp. 1197, 1997.

[30] J. Yue, A. J. Epstein, Z. Zhong, P. K. Gallagher and A. G. MacDiarmid, Synth. Met., vol. 41(1-2), pp. 765, 1991.


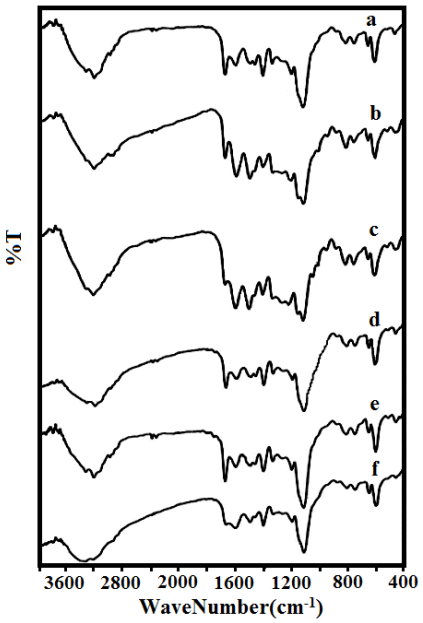


**Fig.1. FT-IR spectra of a) POT 1 b) POT 2 c) POT 3 d) POT 4 e) POT 5 f) POT(undoped)**

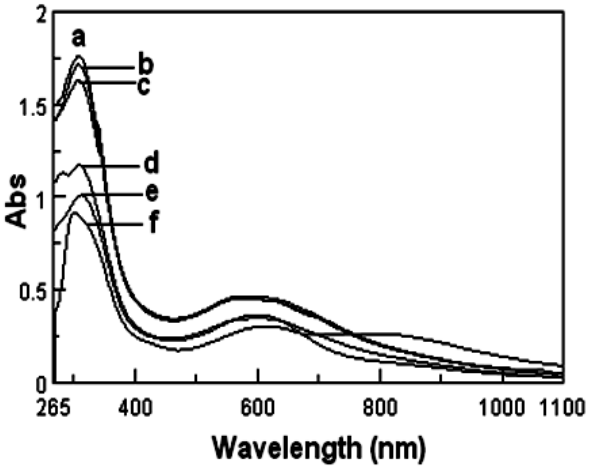


Fig.2. UV-Vis spectra of a) POT 1 b) POT 2 c) POT 3 d) POT 4 e) POT 5 f) POT (undoped)

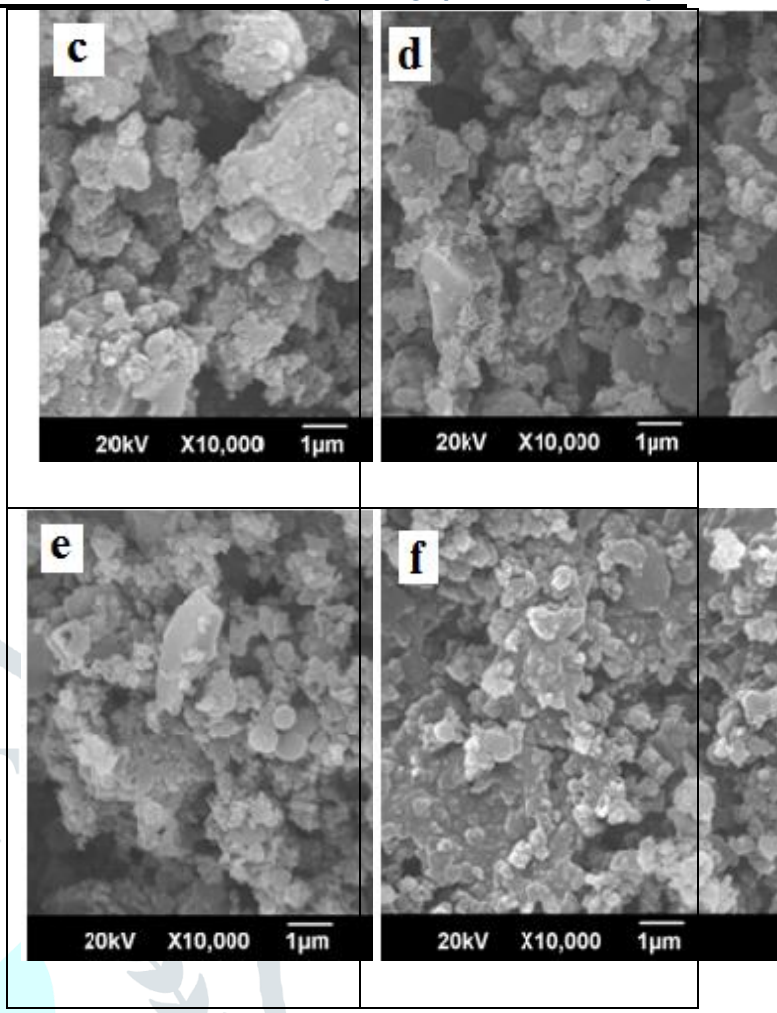


Fig.3. SEM photographs of a) POT (undoped) b) POT 1 c) POT 2 d) POT 3 e) POT 4 f) POT 5

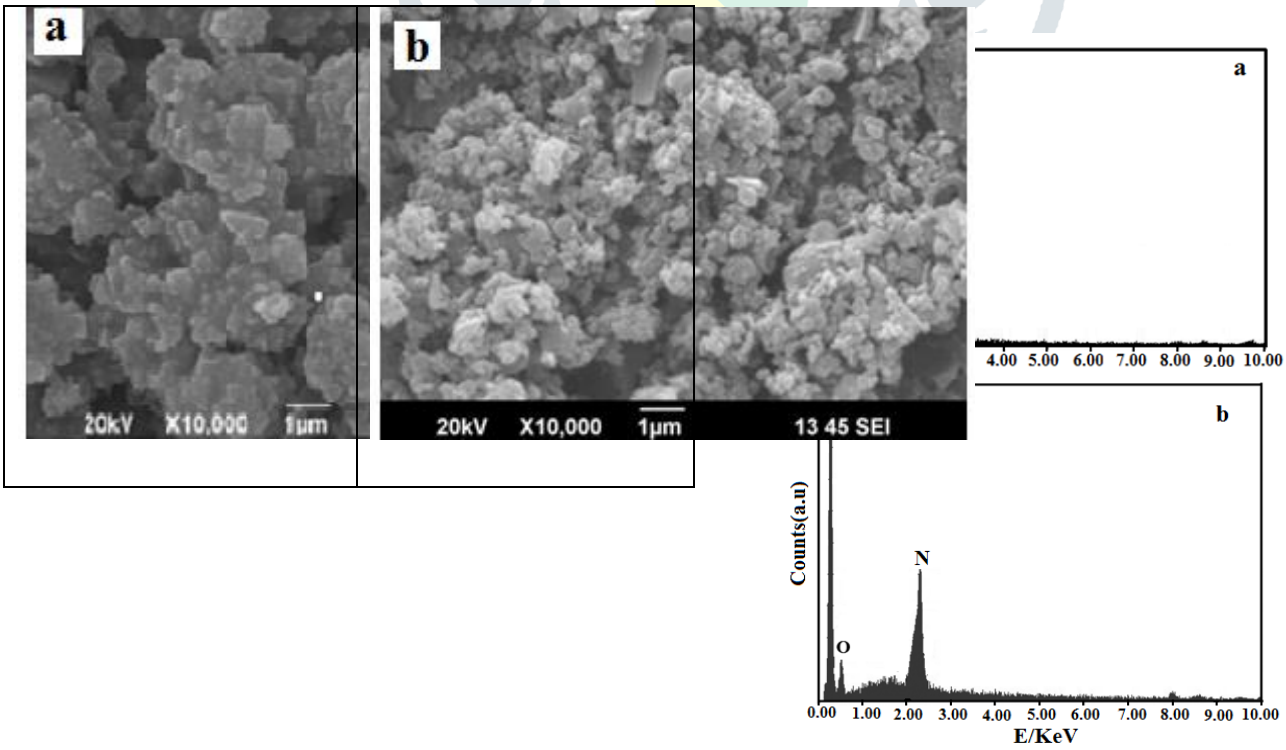


Fig.4. EDAX behaviour of a) POT (undoped) b) POT 1

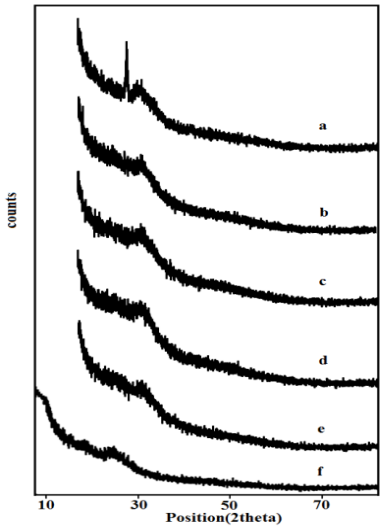


**Fig.5. XRD of a) POT 1 b) POT 2 c) POT 3 d) POT 4 e) POT 5 f) POT (undoped)**

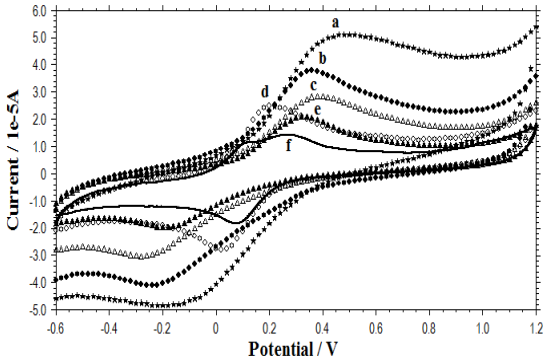


**Fig.6. Cyclic voltammogram of a) POT 1 b) POT 2 c) POT 3 d) POT 4 e) POT 5 f) POT (undoped)**

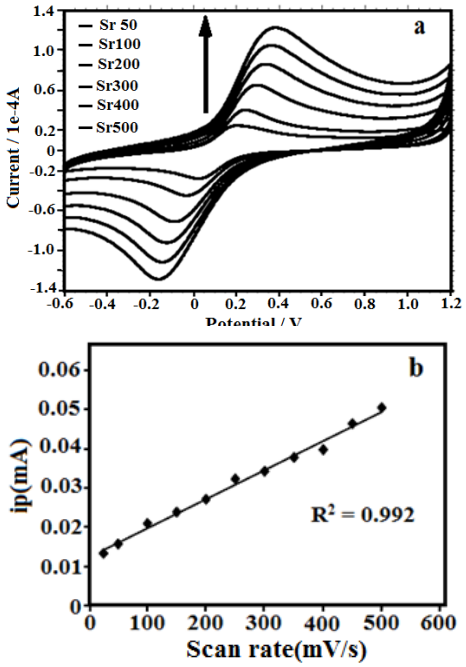


**Fig.7. a) CV taken at various scan rates for POT 1 b) Plot of anodic current Vs scan rate for POT 1**

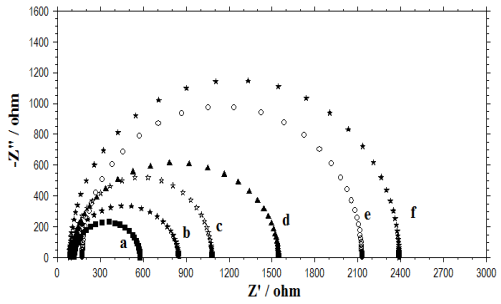


**Fig.8. Impedance spectra of a) POT 1 b) POT 2 c) POT 3 d) POT 4 e) POT 5 f) POT (undoped)**

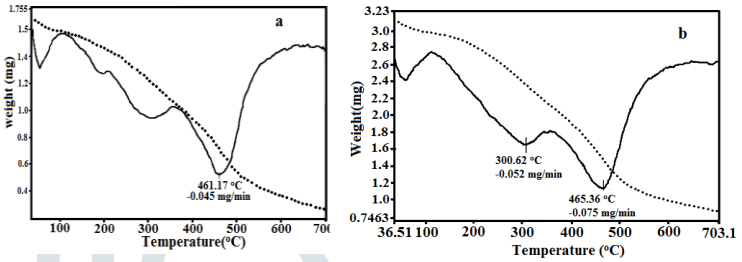


**Fig.9. TGA/DTA image of a) POT (undoped) POT 1**

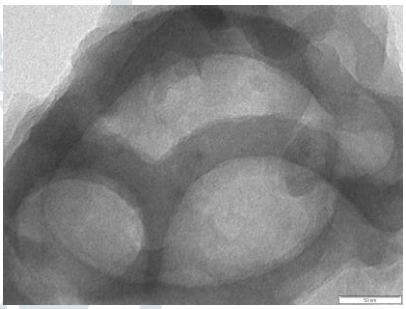

**Fig.10. TEM image of POT 1**